Bias Point Optimisation in LiFi for Capacity Enhancement

Tilahun Zerihun Gutema, *Student Member, IEEE,* Harald Haas, *Fellow, IEEE,* and Wasiu O. Popoola, *Senior Member, IEEE*

***Abstract*—In this paper, we investigate methods to optimise the bias point of an LED to benefit from increasing bandwidth at higher driving current while minimising the resulting signal distortion. The approaches are based on allowing for some nonlinear distortion or to reduce signal swing/signal-to-noise ratio while benefiting from higher bandwidth at higher driving currents. A framework is presented to estimate the attainable capacity under both conditions. We also experimentally validate the optimisation with a PAM-4 based VLC system. The experimental results show that for a 40 mA dynamic range VLMB1500 LED used, the optimum bias point is not in the middle of the dynamic range but at 31 mA.**

***Index Terms*—Visible light communication (VLC), light fidelity (LiFi), light emitting diode (LED), DC bias, pulse amplitude modulation (PAM), orthogonal frequency division multiplexing (OFDM), error vector magnitude (EVM), transmission capacity.**

I. Introduction

THE continued rapid growth of data traffic is demanding high-capacity communication systems. This is driving the radio frequency (RF) based wireless communication towards spectrum shortage [1]. However, in the optical domain, large and unlicensed spectrum, free from electromagnetic interference, and with inherent security is available. This makes optical wireless communication (OWC) a plausible technology to supplement developments in the RF-based networks [2]. Visible light communication (VLC), a subset of OWC, operates in the visible light spectrum and exploits the existing lighting infrastructure for communication. In addition, energy efficient, inexpensive and widely available front-end devices such as light-emitting diodes (LEDs) enable VLC to draw increasing interest for indoor wireless communications [3].

Significant research effort has been put towards the development of high-speed VLC. Yet, such a system needs to address the challenges associated with the relatively low modulation bandwidth of commercial LEDs [4]. Various techniques such as pre- and post-equalisation, high-order modulation with orthogonal frequency division multiplexing (OFDM) have been explored to optimise the modulation bandwidth and achieve high data rates in the range of several Gb/s using a single LED [5], [6]. It has also been demonstrated that the LED modulation bandwidth increases as bias current increases until it saturates [7], [8]. However, an LED is a nonlinear device. That is, its emitted optical power as a function of the driving current is not completely linear. Consequently, driving the LED in the nonlinear region distorts the transmitted signal and deteriorates the system performance [9]. Therefore, it is imperative to optimise the DC bias point of an LED to benefit from increasing bandwidth at driving current while minimising any nonlinear distortion associated with operating beyond the dynamic range of the LED. This way, the achievable transmission capacity of the LED based VLC system is enhanced.

Related work on VLC capacity optimisation includes the following: a pre-distortion technique combined with signal shaping is used to improve the link capacity in [10], by pre-distorting and DC-biasing, the transmitted signal is optimised to increase the capacity of the system. In [11], to maximise the system performance, a low complexity search algorithm is developed that finds the optimum biasing point by enhancing the effective signal-to-noise ratio (SNR) of the system. In [12], a numerical method based on minimising mean squared error (MMSE) criterion is proposed to optimise the DC bias that improves the bit error rate (BER) performance.

Most of the existing works considered pre-distortion to linearise the dynamic range of the transmitted or apply clipping to limit the modulating signal in the linear region [10]–[12]. In this paper, we investigate two different methods of choosing the optimum DC bias point for intensity modulated VLC systems. The first approach considers increasing the DC bias from the mid-point of the linear region for higher modulation bandwidth which also leads to nonlinear distortion. Here, the effect of distortion on the system capacity is evaluated. The second approach investigates increasing the DC bias while keeping the modulating signal within the dynamic range of the transmitter. In this approach, the signal power is compressed, and the optical modulation index is reduced. As such, the SNR decreases as DC bias increases. Thus, the optimum DC bias that provides maximum capacity by increasing the modulation bandwidth is evaluated. Moreover, these optimisation techniques can be used together with existing pre/post equalisation and precoding/pre-distortion techniques. We also present an experimental validation of the optimisation.

The remainder of the paper is organised as follows. The system design and principle of the bias optimisation methods is discussed in Section II. Section III presents the simulation results, discussions as well as the experimental validation of the optimisation. Finally, concluding remarks are provided in

Tilahun Zerihun Gutema and Wasiu O. Popoola are with the Institute for Digital Communications, School of Engineering, The University of Edinburgh, Edinburgh, EH9 3FD, UK (e-mail: tilahun.gutema@ed.ac.uk; w.popoola@ed.ac.uk).

Harald Haas is with University of Strathclyde, The Technology and Innovation Centre, 99 George Street, Glasgow, G1 1RD, U.K. (e-mail: harald.haas@strath.ac.uk)

Section IV.

II. System Design

This section presents the DC bias point optimisation problem as well as the VLC system model.

A considerable amount of nonlinearity in VLC systems comes from the LED. That is because the relationship between the DC bias current and the output optical power is not linear. Thus, to minimise the effect of nonlinearity distortion on VLC systems, the data carrying signal should be within the linear dynamic range of the LED [13]. This is usually achieved by biasing the LED at the mid-point of its dynamic range [14]. In this work, we explore two different approaches of choosing the DC bias (operating) point. In the first approach, the modulating signal amplitude is kept constant while the bias current is increased from the mid-point of the dynamic range. In this approach, some of the signal go into the nonlinear region, introducing some distortion but operating at higher bias current offers much higher bandwidth. The second approach will be to increase the bias point while keeping the signal within the dynamic range of the LED. Thus, the signal power is reduced while the bandwidth is increased. In these methods, the response of the LED is considered to be distortion free. The challenge in both methods is to find the optimum DC bias point that maximises the link capacity. Other sources of distortions are not considered in this work. So, the modulating signal bandwidth is assumed to be less than the LED bandwidth. Furthermore, these bias optimisation methods are applied considering the commercially available VLMB1500 LED as an access point. The methods can be applied to the user-end devices independently using the same process.

A. VLC Model and Link Capacity

An intensity modulation VLC channel can be modelled as a baseband linear, time-invariant system as shown in Fig. 1 [15]. In this model, $x\left(t\right)$ denotes the input modulating electrical signal and the output photodetector current is represented by $y\left(t\right)$. The channel impulse response is $h\left(t\right)$ with its corresponding frequency response, $H\left(f\right) = \int_{-\infty}^{\infty} h\left(t\right) \mathrm{e}^{-\mathrm{j}2\pi ft} dt$. For indoor VLC, the line-of-sight link is dominant and the channel can be well-characterised by its DC gain, $H\left(0\right)$ [16], [17].

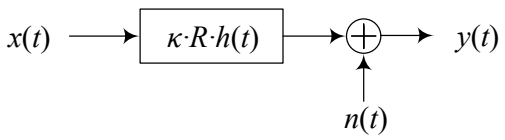

Fig. 1. Channel model with modulating signal $x\left(t\right)$, output photodetector current $y\left(t\right)$, additive noise $n(t)$, and an impulse response $h\left(t\right)$. R represents the responsivity of the photodetector while κ is LED's electrical-to-optical conversion factor.

Consequently, the equivalent received signal can be summarised by:

$$y\left(t\right) = \kappa R\left(h\left(t\right) * x\left(t\right)\right) + n\left(t\right). \tag{1}$$

Here "$*$" symbol denotes the convolution operation, κ is the electrical-to-optical conversion factor of LED in W/A, and R is the responsivity of the photodetector.

The two primary sources of noise in VLC are due to random photon fluctuation of the received photocurrent (shot noise) and noise from the receiver electronics (thermal noise). The variance of the shot noise can be estimated by [18]:

$$\sigma_{\text{shot}}^2 = 2qRP_{\text{opt}}B, \tag{2}$$

where the electron charge is denoted by q, and P_{opt} is the received average optical power at the photodetector. The transmission bandwidth is denoted by B. The thermal noise is given as [18]:

$$\sigma_{\text{thermal}}^2 = \frac{4\mathrm{K_B}TB}{R_{\mathrm{L}}}, \tag{3}$$

where $\mathrm{K_B}$ is the Boltzmann's constant, T is the operating temperature in Kelvin. The load resistance is denoted by R_{L}. Both shot noise and thermal noise can be considered as white and Gaussian [18], and independent of transmitted optical power. Hence, it is acceptable to model $n\left(t\right)$ as additive white Gaussian noise (AWGN) with total noise variance written as:

$$\sigma_{\mathrm{n}}^2 = \sigma_{\text{shot}}^2 + \sigma_{\text{thermal}}^2. \tag{4}$$

B. Bias Point Optimisation

Two different biasing methods are examined to evaluate the effect on SNR and consequently the capacity of the link. In the first method (*Method* 1, hereafter), the effect of distortion on SNR is studied by increasing the bias current and driving the LED into saturation region. In the second method (*Method* 2, hereafter), the LED is operating in the non-saturation region by compressing the modulating signal within the linear region. In this method, the result of squeezing the signal in linear region on SNR is studied as the driving current is increased. A visual illustration of an LED response using a random modulating signal, $x\left(t\right)$ is shown in Fig. 2. The LED is biased at i_{bias} by adding an offset current α to the mid-point bias current i_{mid}.

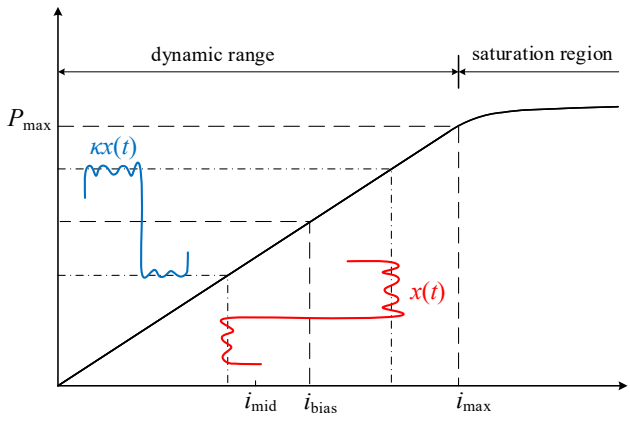

Fig. 2. Graphical illustration of an LED response biased at i_{bias} using a random modulating signal, $x\left(t\right)$. The maximum allowable bias current of the LED is i_{max} and the mid-point is $i_{\text{mid}} = i_{\text{max}}/2$.

The transmission bandwidth of the VLC link and the optical power output of the LED are a function of the bias current.

This relationship between bandwidth and bias current is linear. Therefore, it can be formulated as:

$$B = \begin{cases} m_B i_{\text{bias}}, & \text{for } i_{\text{mid}} \leq i_{\text{bias}} < i_{\max_{\text{B}}} \\ B_{\max}, & \text{for } i_{\text{bias}} \geq i_{\max_{\text{B}}}. \end{cases} \tag{5}$$

Similarly, the relationship between optical power and bias current is linear and can be written as:

$$P_{\text{opt}} = \begin{cases} m_O i_{\text{bias}}, & \text{for } i_{\text{mid}} \leq i_{\text{bias}} < i_{\max_{\text{P}}} \\ P_{\max}, & \text{for } i_{\text{bias}} \geq i_{\max_{\text{P}}}. \end{cases} \tag{6}$$

Here, m_B and m_O denote the slopes of the linear functions of the dynamic ranges with a maximum bandwidth, $B_{\max}$ at drive current $i_{\max_{\text{B}}}$ and maximum power, $P_{\max}$ at drive current $i_{\max_{\text{P}}}$, respectively. For most LEDs $i_{\max_{\text{B}}} = i_{\max_{\text{P}}} = i_{\max}$ as verified in Section III.

1) Method 1: Bias Optimisation with Constant Signal Amplitude and Distortion: due to the modulation of LED into the nonlinear region, the transmitted signal is distorted. The amount of distortion can be estimated as a ratio of power in saturation region to the total signal power. Therefore, the distortion factor, Δ, can be expressed as a function of the bias point, $i_{\text{bias}} = i_{\text{mid}} + \alpha$, as:

$$\Delta\left(i_{\text{bias}}\right) = \frac{\int_{i_{\max}}^{i_{\max}+\alpha} x^2 f\left(x\right) dx}{\int_{-\infty}^{\infty} x^2 f\left(x\right) dx}, \tag{7}$$

where $f\left(x\right)$ is the probability density function (pdf) of $x(t)$, $i_{\max}$ is the maximum allowable drive current before saturation and α is offset from the mid-point current, i_{mid}, as shown in Fig. 2. In this equation, the numerator represents the signal power loss due to distortion while the denominator represents the total signal power. For simplicity, we use the zeroth moment expressions of (7) which can be simplified to ratio of two cumulative distribution functions as:

$$\Delta\left(i_{\text{bias}}\right) \approx \frac{\int_{i_{\max}}^{i_{\max}+\alpha} f\left(x\right) dx}{\int_{-\infty}^{\infty} f\left(x\right) dx}. \tag{8}$$

For a Gaussian distributed signal $x(t)$, the values of equations (7) and (8) are plotted in Fig. 3 to illustrate the validity of the approximation. It shows that up to 35 mA bias current, equations (7) and (8) have similar values and above 35 mA equation (8) underestimates the distortion by less than 4%.

The electrical SNR of the VLC model with distortion can then be expressed as:

$$\text{SNR}_{\text{M1}}\left(i_{\text{bias}}\right) = \frac{\kappa^2 R^2 H^2(0)\left(1-\Delta\right)\text{E}\left[\left|x\left(t\right)\right|^2\right]}{\sigma_{\text{n}}^2 + \kappa^2 R^2 H^2(0)\Delta\text{E}\left[\left|x\left(t\right)\right|^2\right]}, \tag{9}$$

where $H\left(0\right) = \int_{-\infty}^{\infty} h\left(t\right) dt$ is the channel DC gain, and $\text{E}\left[\cdot\right]$ denotes the statistical expectation. The second term in the denominator accounts for the distorted signal power.

For a VLC system with sufficient DC bias and a Gaussian distributed $x(t)$, the link capacity is adequately represented by the Shannon-Hartley equation given by $C = B\log_2\left(1+\text{SNR}\right)$. Therefore, for *Method* 1, the link capacity as a function of bias current $C_{\text{M1}}\left(i_{\text{bias}}\right)$ is obtained by combining (2), (3), (4), (5), (6), and (9) as shown in (10).

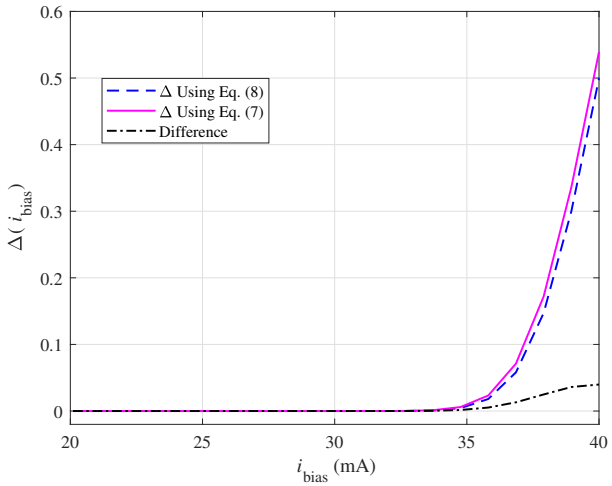

Fig. 3. Distortion factor, Δ as function of i_{bias} using equations (7) and (8).

2) Method 2: Bias optimisation with no distortion: here the bias current is increased while the signal is compressed within the linear region of the LED. The signal scaling factor, γ is used to keep the modulating signal within the linear dynamic range of the LED. As a function of bias current, γ can be written as:

$$\gamma\left(i_{\text{bias}}\right) = \begin{cases} \frac{i_{\max}-i_{\text{bias}}}{\max|x(t)|}, & \text{if } \max|x(t)| > i_{\max} - i_{\text{bias}} \\ 1, & \text{otherwise.} \end{cases} \tag{11}$$

In *Method* 2, as the signal, $x(t)$, is constrained to the linear region only, there is negligible distortion. Thus, the electrical SNR is reduced to:

$$\text{SNR}_{\text{M2}}\left(i_{\text{bias}}\right) = \frac{\kappa^2 R^2 H^2\left(0\right)\gamma^2\text{E}\left[\left|x\left(t\right)\right|^2\right]}{\sigma_{\text{n}}^2}. \tag{12}$$

Similar to *Method* 1, the link capacity as a function of the bias current for *Method* 2, $C_{\text{M2}}\left(i_{\text{bias}}\right)$ is obtained as shown in (13).

$$C_{\text{M2}} = m_B i_{\text{bias}} \log_2\left(1 + \frac{\kappa^2 R^2 H^2\left(0\right)\gamma^2\text{E}\left[\left|x\left(t\right)\right|^2\right]}{2\left(qRm_O i_{\text{bias}} + \frac{2\text{K}_{\text{B}}T}{R_{\text{L}}}\right)m_{\text{B}} i_{\text{bias}}}\right). \tag{13}$$

The link capacity expressions (10) and (13) are a product of a monotonically increasing linear function and a decreasing logarithmic function. Hence, there exist an optimum bias current, $\hat{i}_{\text{bias}}$, which provides maximum link capacity. This optimum bias current with $i_{\text{mid}} \leq \hat{i}_{\text{bias}} < i_{\max}$ will satisfy:

$$\frac{\partial C_{\text{M1|2}}\left(i_{\text{bias}}\right)}{\partial i_{\text{bias}}} = 0 \quad \text{and} \quad \frac{\partial^2 C_{\text{M1|2}}\left(i_{\text{bias}}\right)}{\partial i_{\text{bias}}^2} < 0. \tag{14}$$

The authors are unaware of a closed-form analytical solution to (14). However, a solution can be obtained with root-finding numerical methods. Moreover, to show the effect of the bias current on achievable capacity, a graphical solution of (14) is explored.

III. Results, Discussion and Experimental Validation

This section presents simulation results of the bias optimisation methods as well as an experimental validation of a PAM based VLC system using *Method* 2. In the simulation, a commercially available off-the-shelf LED VLMB1500 is used [19]. Its optical power and electrical bandwidth response using a pulse signal is characterised and presented in Fig. 4. The results show that the maximum allowable bias current before saturation in power and bandwidth is 40 mA for this particular LED.

A. Simulation Results

For the simulation example presented here, a maximum drive current of 40 mA is considered based on the VLMB1500 LED whose characteristics are plotted in Fig. 4. The bias current is started from the mid-point (20 mA) and increased to the maximum (40 mA) aiming to graphically determine the optimum drive current which provides maximum capacity. The simulation parameters are summarised in Table I.

TABLE I
Simulation Parameters

Parameter	Value
Average transmitted signal power, $\mathrm{E}\left[\lvert x(t)\rvert^2\right]$	1 W
Maximum allowable bias current, $i_{\max}$	40 mA
Slope of the dynamic range (bandwidth), m_{B}	370.30 MHz/A
Slope of the dynamic range (power), m_{O}	14.15 mW/A
Maximum bandwidth, $B_{\max}$	23.952 MHz
Maximum optical power, $P_{\max}$	0.6838 mW
Responsivity of LED, κ	14.15 mW/A
Channel DC Gain, $H(0)$	1
Responsivity of photodetector, R	0.28 A/W
Electron charge, q	1.6021×10^{-19} C
Boltzmann's constant, $\mathrm{K_B}$	1.3806×10^{-23} J/K
Absolute temperature, T	300 K
Load resistance, R_{L}	50 Ω

Fig. 5 shows the capacity as the bias current is increased in *Method* 1 and *Method* 2. The optimum bias point, for maximum capacity with *Method* 1, is obtained at 27.4 mA. This shows that the gain from the linear increment in the electrical bandwidth is not sufficient to compensate for the distortion of signal power beyond this optimum point. However, in *Method* 2, the capacity increases as bias current increases until the optimum bias point is 33.7 mA (Numerical solution of (14) gives a solution of 33.5 mA). Both approaches record identical maximum capacity for the parameters used. But, in terms of efficient use of the available bandwidth at their respective optimum bias points, *Method* 1 is preferable with 30.6 bit/s/channel use as against 27.5 bits/s/channel use for *Method* 2. However, data transmission that uses *Method* 1 must be able to cope with any distortions introduced by this method or high transmission error rate will ensue. Note that the results in Fig. 5 provide the maximum achievable information rate using a Gaussian distributed signal and AWGN channel. For commonly used modulation formats, there will always be a performance gap from the maximum capacity predicted by (10) and (13). This capacity gap can be approached through probabilistic symbol shaping and channel coding [20].

B. Experimental Validation

In this section, the experimental validation of *Method* 2 is presented. We choose this method as it benefits more from the linear increase of modulation bandwidth as the DC bias is increased and there is no nonlinear distortion to contend with. Furthermore, for illustration purpose and simplicity, PAM based VLC is implemented in the experiment.

A block diagram of the experimental setup is shown in Fig. 6. At the transmitter side, uniformly distributed random integers are generated and mapped into PAM-4 symbols. After up-sampling by oversampling factor of 4, rectangular pulse shaping is applied to generate pulse signal. This offline signal generation is done in MATLAB. The pattern is then uploaded to an arbitrary waveform generator (AWG: Keysight 33622A) to generate RF modulating signal. The sampling rate in the range of 40 MSa/s to 200 MSa/s are used in performance evaluation. The output of the AWG and the DC bias current from a DC power supply are combined using a bias-tee (Bias-T: Mini-Circuits ZFBT-4R2GW+). The output signal from the bias-tee is connected to the LED (VLMB1500-GS08). Since the half-power semi-angle of the LED is wide (i.e. about 65° [19]), aspheric condenser lenses (Thorlabs ACL4532) are used to collimate the output light from the transmitter and focus it into the detection area of the photodetector.

At a receiver side with a link distance of 0.5 m, a photodetector (PD: ThorLabs PDA10A) is used to detect the intensity modulated signal. The receiver has a -3 dB bandwidth of 150 MHz and a built-in transimpedance amplifier (TIA) with a gain of 5 V/mA. The received electrical signal is captured by an oscilloscope (OSC: Keysight MSO7104B) followed by offline processing in MATLAB. The post-processing includes alignment of received signal to transmitted, normalisation of the amplitude level, and matched filtering. For performance evaluation, the root-mean-square (RMS) error vector magnitude (EVM) is measured for different sampling rates of transmission.

$$C_{\mathrm{M1}} = \begin{cases} m_B i_{\mathrm{bias}} \log_2\left(1+\dfrac{\kappa^2R^2H^2(0)(1-\Delta)\mathrm{E}\left[|x(t)|^2\right]}{2\left(qRm_O i_{\mathrm{bias}}+\frac{2\mathrm{K_B}T}{R_{\mathrm{L}}}\right)m_{\mathrm{B}}i_{\mathrm{bias}}+\kappa^2R^2H^2(0)\Delta\mathrm{E}\left[|x(t)|^2\right]}\right), & \text{for } i_{\mathrm{mid}} \le i_{\mathrm{bias}} < i_{\max} \\ B_{\max}\log_2\left(1+\dfrac{\kappa^2R^2H^2(0)(1-\Delta)\mathrm{E}\left[|x(t)|^2\right]}{2\left(qRP_{\max}+\frac{2\mathrm{K_B}T}{R_{\mathrm{L}}}\right)B_{\max}+\kappa^2R^2H^2(0)\Delta\mathrm{E}\left[|x(t)|^2\right]}\right), & \text{for } i_{\mathrm{bias}} \ge i_{\max}. \end{cases} \tag{10}$$

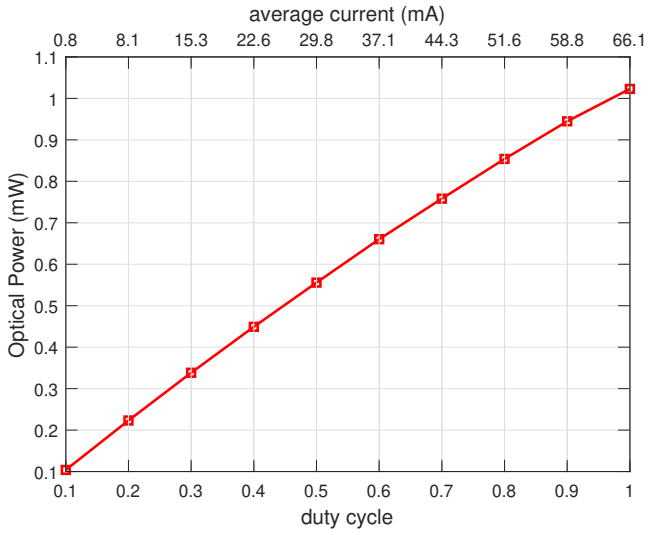

Fig. 4. Characteristics of VLMB1500 LED at different bias current showing (a) measured output optical power using a pulse signal and (b) measured -3 dB electrical bandwidth and linear fit with $R^2 = 0.99987$.

Having determined the dynamic range of the LED as shown in Fig. 4, to validate the optimum biasing point which provides maximum capacity, five different biasing points are considered in a transmission experiment. These biasing points are all within the dynamic range of the LED. For each of these biasing points, the modulating PAM signal is scaled to fit the linear operating region of the LED. This is achieved by adjusting the peak-to-peak voltage $(V\text{pp})$ output of the AWG. These values are, $V\text{pp} = [540, 360, 240, 120, 40]$ mV at bias currents, $i_{\text{bias}} = [20, 25, 30, 35, 38]$ mA, respectively.

To investigate the achievable transmission rate, the EVM metric at different sampling rates of the AWG are measured for all biasing points. The result is depicted in Fig. 7. It can be seen that the EVM performance gets better when biasing current is increased from 20 mA to 30 mA and gets worse at higher biasing currents.

The performance is further demonstrated in Fig. 8 where the maximum sampling rates attainable at two EVM values are by

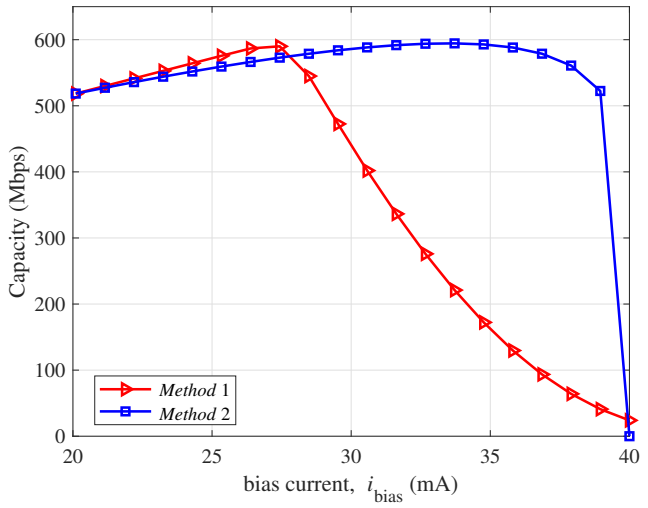

Fig. 5. Simulation results of capacity with different bias current for *Method* 1 and *Method* 2 using OFDM modulation scheme.

plotting against the bias current. In choosing these reference EVM values, the hard decision forward error correction (HD-FEC) threshold of BER $\leq 3.8 \times 10^{-3}$ is considered. The equivalent EVM of 25% or lower is obtained by applying EVM $= 1/\sqrt{\text{SNR}}$ and the theoretical PAM-4 BER expression, $P_b = \frac{1}{4}\left(3Q\left(\sqrt{\frac{2}{5}\text{SNR}}\right) + 2Q\left(3\sqrt{\frac{2}{5}\text{SNR}}\right)\right)$, where $Q(\cdot)$ is the Gaussian Q-function.

The result shows that a maximum sampling rate of 190 MSa/s, equivalent to 95 Mbit/s, is attained at 30 mA. This is an increase from 140 MSa/s (equivalent to 70 Mbit/s) when the LED is biased at 20 mA, in the middle of its dynamic range. In terms of spectral efficiency at the reference EVM for the PAM-4, 30 mA biasing provides 4.7 bit/s/channel use, higher than at other bias points. Thus, from the polynomial fit in Fig. 8, the optimum bias point is not in the middle of the dynamic range but at 31 mA. This agrees quite closely with the 33.7 mA obtained from the simulation. This validates the simulation result of *Method* 2 bias optimisation discussed in the previous subsection. Thus, by using the optimum DC biasing and keeping the modulating signal power within the LED's dynamic range, transmission with higher rate can be attained and consequently the link capacity is enhanced.

IV. Conclusion

It has been shown that the modulation bandwidth of an LED increases at the DC bias from the mid-point of its linear region. We then consider the effect of this on the received SNR and report on two techniques for choosing the optimum DC bias point that maximises the link capacity. In the first approach, as the bias point is increased the input signal swing is allowed into the saturation region of the LED. The resulting distortion causes a decrease in the SNR. In the second method, the inputs signal is constrained to the LED dynamic range with no nonlinear distortion. Simulation results of attainable capacity from the two methods is presented. The simulation results show that the optimum bias point does not lie in the middle of the dynamic range. This is further validated with

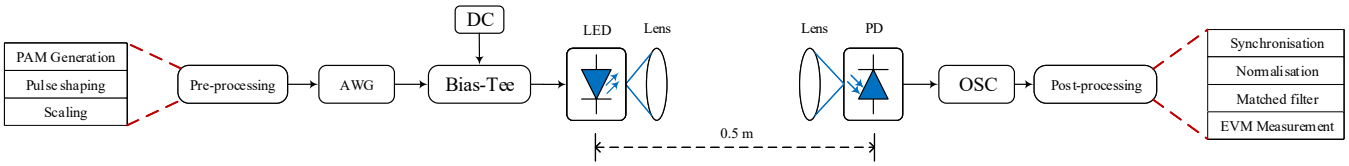

Fig. 6. The block diagram of the experimental setup

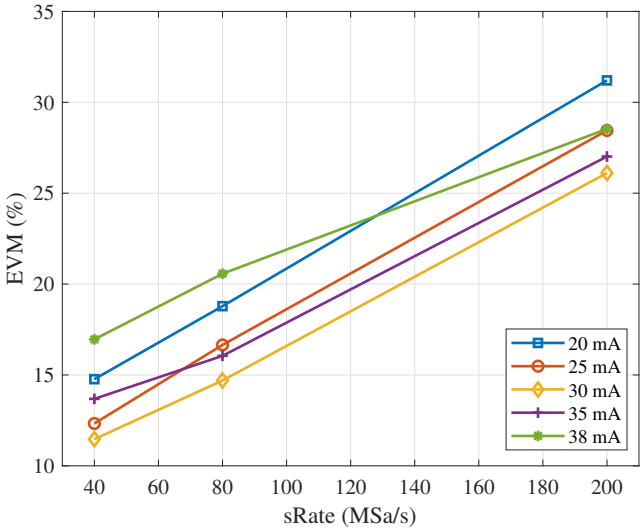

Fig. 7. Performance of the link in terms of EVM for different sampling rates

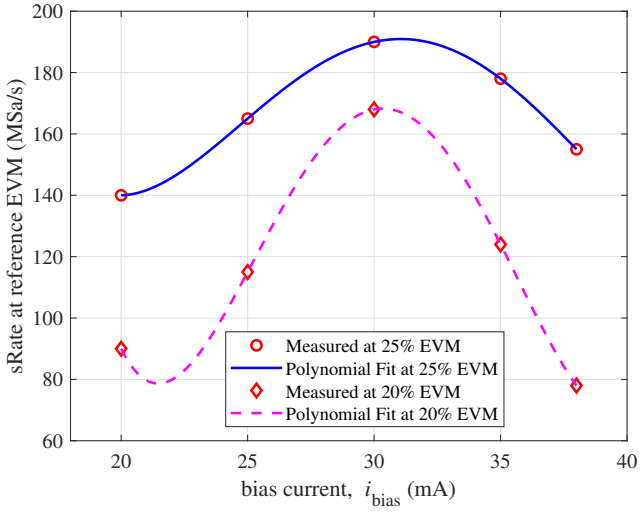

Fig. 8. Achieved sampling rates using 25% and 20% reference EVM at different bias current

a PAM based VLC experiment. Experimental results show that by increasing the bias current from the mid-point of the linear region, 20 mA, to the optimum bias current, 30 mA, the transmission rate can be increased by $\sim 36\%$. The presented optimisation approaches can be combined with the existing pre/post equalisation and precoding/pre-distortion techniques for higher gains.

ACKNOWLEDGEMENT

This work is funded by the European Union's Horizon 2020 research and innovation programme under the Marie Skłodowska Curie grant agreement №. 814215 titled ENLIGHT'EM: European Training Network in Low-Energy Visible Light IoT Systems: https://enlightem.eu/

REFERENCES

[1] T. Cogalan and H. Haas, "Why would 5G need optical wireless communications?" in *2017 IEEE 28th Annual International Symposium on Personal, Indoor, and Mobile Radio Communications (PIMRC)*. IEEE, 2017, pp. 1–6.

[2] T. Koonen, "Indoor Optical Wireless Systems: Technology, Trends, and Applications," *Journal of Lightwave Technology*, vol. 36, no. 8, pp. 1459–1467, 2018.

[3] D. Karunatilaka, F. Zafar, V. Kalavally, and R. Parthiban, "LED based indoor visible light communications: State of the art," *IEEE Communications Surveys & Tutorials*, vol. 17, no. 3, pp. 1649–1678, 2015.

[4] W. O. Popoola, E. Poves, and H. Haas, "Error performance of generalised space shift keying for indoor visible light communications," *IEEE Transactions on Communications*, vol. 61, no. 5, pp. 1968–1976, 2013.

[5] D. Tsonev, H. Chun, S. Rajbhandari, J. J. McKendry, S. Videv, E. Gu, M. Haji, S. Watson, A. E. Kelly, G. Faulkner *et al.*, "A 3-Gb/s single-LED OFDM-Based wireless VLC link using a Gallium Nitride μLED," *IEEE Photonics Technology Letters*, vol. 26, no. 7, pp. 637–640, 2014.

[6] X. Huang, S. Chen, Z. Wang, J. Shi, Y. Wang, J. Xiao, and N. Chi, "2.0-Gb/s visible light link based on adaptive bit allocation ofdm of a single phosphorescent white led," *IEEE Photonics Journal*, vol. 7, no. 5, pp. 1–8, 2015.

[7] G. Stepniak, J. Siuzdak, and P. Zwierko, "Compensation of a VLC phosphorescent white LED nonlinearity by means of volterra DFE," *IEEE Photonics Technology Letters*, vol. 25, no. 16, pp. 1597–1600, 2013.

[8] P. Deng, M. Kavehrad, and M. A. Kashani, "Nonlinear modulation characteristics of white LEDs in visible light communications," in *Optical Fiber Communication Conference*. Optical Society of America, 2015, pp. W2A–64.

[9] B. Inan, S. J. Lee, S. Randel, I. Neokosmidis, A. M. Koonen, and J. W. Walewski, "Impact of LED nonlinearity on discrete multitone modulation," *Journal of Optical Communications and Networking*, vol. 1, no. 5, pp. 439–451, 2009.

[10] S. Dimitrov and H. Haas, "Optimum signal shaping in OFDM-based optical wireless communication systems," in *2012 IEEE Vehicular Technology Conference (VTC Fall)*. IEEE, 2012, pp. 1–5.

[11] L. Chen, B. Krongold, and J. Evans, "Performance evaluation of optical OFDM systems with nonlinear clipping distortion," in *2009 IEEE International Conference on Communications*. IEEE, 2009, pp. 1–5.

[12] M. Zhang and Z. Zhang, "An optimum DC-biasing for DCO-OFDM system," *IEEE Communications Letters*, vol. 18, no. 8, pp. 1351–1354, 2014.

[13] K. Ying, Z. Yu, R. J. Baxley, H. Qian, G.-K. Chang, and G. T. Zhou, "Nonlinear distortion mitigation in visible light communications," *IEEE Wireless Communications*, vol. 22, no. 2, pp. 36–45, 2015.

[14] Y. Hei, Y. Kou, G. Shi, W. Li, and H. Gu, "Energy-spectral efficiency tradeoff in DCO-OFDM visible light communication system," *IEEE Transactions on Vehicular Technology*, vol. 68, no. 10, pp. 9872–9882, 2019.

[15] J. M. Kahn and J. R. Barry, "Wireless infrared communications," *Proceedings of the IEEE*, vol. 85, no. 2, pp. 265–298, 1997.

[16] L. Zeng, D. C. O'Brien, H. Le Minh, G. E. Faulkner, K. Lee, D. Jung, Y. Oh, and E. T. Won, "High data rate multiple input multiple output (mimo) optical wireless communications using white led lighting," *IEEE Journal on Selected Areas in Communications*, vol. 27, no. 9, pp. 1654–1662, 2009.
[17] C. Chen, M. Ijaz, D. Tsonev, and H. Haas, "Analysis of downlink transmission in dco-ofdm-based optical attocell networks," in *2014 IEEE global communications conference*. IEEE, 2014, pp. 2072–2077.
[18] Z. Ghassemlooy, W. Popoola, and S. Rajbhandari, *Optical wireless communications: system and channel modelling with Matlab®*. CRC press, 2019.
[19] *Ultrabright 0402 ChipLED*, Vishay, Feb. 2017.
[20] G. D. Forney and G. Ungerboeck, "Modulation and coding for linear gaussian channels," *IEEE Transactions on Information Theory*, vol. 44, no. 6, pp. 2384–2415, 1998.

Tilahun Zerihun Gutema Tilahun Zerihun Gutema received the B.Sc. degree in electrical engineering from Addis Ababa University, Addis Ababa, Ethiopia in 2015, and the M.Sc. degree in optics and photonics, from Karlsruhe Institute of Technology, Karlsruhe, Germany, in 2018. He is currently working toward the Ph.D. degree in digital communications at the University of Edinburgh, U.K. His main research interest is in visible light communication.

Harald Haas (FREng FRSE FIEEE FIET) received the Ph.D. degree from The University of Edinburgh in 2001. He is a Distinguished Professor of Mobile Communications at the University of Strathclyde and the Director of the LiFi Research and Development Centre. He also set-up and co-founded pureLiFi Ltd which it currently serves as Chief Scientific Officer. He has authored over 550 conference and journal papers. Haas' main research interests are in optical wireless communications, hybrid optical wireless and RF communications, spatial modulation, and interference coordination in wireless networks. His team invented spatial modulation. He introduced LiFi to the public at an invited TED Global talk in 2011. LiFi was listed among the 50 best inventions in TIME Magazine in 2011. In 2016, he received the Outstanding Achievement Award from the International Solid State Lighting Alliance. In 2019 he was recipient of IEEE Vehicular Society James Evans Avant Garde Award. Haas was elected a Fellow of the Royal Society of Edinburgh (RSE) in 2017. In the same year he received a Royal Society Wolfson Research Merit Award and was elevated to IEEE Fellow. In 2018 he received a three-year EPSRC Established Career Fellowship extension and was elected Fellow of the IET. Haas was elected Fellow of the Royal Academy of Engineering (FREng) in 2019.

Wasiu O. Popoola (S'05–A'12–M'13–SM'16) is currently a University Senior Lecturer and Deputy Director of Learning and Teaching at the School of Engineering, University of Edinburgh, U.K. He has published over 110 journal articles/conference articles/patent and over seven of those are invited articles. He also co-authored the book Optical Wireless Communications: System and Channel Modeling with MATLAB and many other book chapters. His primary research interests are digital and optical communications, including VLC, FSO, and fiber communications. One of his journal articles ranked No. 2 in terms of the number of full text downloads within IEEE Xplore, in 2008, from the hundreds of articles published by IET Optoelectronics, since 1980. Another article he co-authored with one of his Ph.D. students received the Best Poster Award at the 2016 IEEE ICSAE Conference.

Popoola is a science communicator appearing in science festivals and on 'BBC Radio 5live Science' programme in Oct. 2017. His publications have over 5600 citations and an h-index of 32 on Google Scholar. He is a senior member of IEEE, an associate editor of the IEEE Access journal and a Fellow of the Higher Education Academy (FHEA). He was an Invited speaker at various events including the 2016 IEEE Photonics Society Summer Topicals.